nature photonics

SUPPLEMENTARY INFORMATION

DOI: 10.1038/NPHOTON.2009.137

Jessie Rosenberg, Qiang Lin, Oskar Painter*

Department of Applied Physics, California Institute of Technology, Pasadena, CA 91125

(Dated: June 20, 2009)

Abstract

We present in this supplement to our manuscript entitled, "Static and Dynamic Wavelength Routing via the Gradient Optical Force," the detailed analysis related to the cavity response in the pump-probe scheme, the anti-crossing of cavity modes, and the calibration of thermo-optic and thermo-mechanical contributions to the cavity resonance tuning.

PACS numbers:

DOI: 10.1038/NPHOTON.2009.137

I. THE CAVITY RESPONSE IN THE PUMP-PROBE SCHEME

Here we provide the derivation of the cavity response in a pump-probe scheme where the mechanical motion is primarily actuated by an intense pump and is experienced by a weak probe at a different resonance frequency.

A. Pump field modulation

In general, the pump wave inside the cavity satisfies the following equation:

$$\frac{da_p}{dt} = (i\Delta_p - \frac{\Gamma_{\rm tp}}{2})a_p - ig_{\rm OM}xa_p + i\gamma|a_p|^2a_p + i\sqrt{\Gamma_{\rm ep}}A_{\rm p}, \tag{S1}$$

where a_p and A_p are the intracavity and input field of the pump wave, respectively, normalized such that $U_p \equiv |a_p|^2$ and $P_p \equiv |A_p|^2$ represent the intracavity energy and input power. $\Delta_p = \omega_p - \omega_{0\rm p}$ represents the detuning of pump frequency ω_p to the cavity resonance $\omega_{0\rm p}$ and $\Gamma_{\rm tp}$ is the photon decay rate of the loaded cavity for the pump mode. In Eq. (S1), the third term represents the back action of mechanical motion on the cavity resonance, where $g_{\rm OM}$ is the optomechanical coupling coefficient and $x(t)$ is the mechanical displacement of the cavity structure. The fourth term describes the self-phase modulation introduced by the Kerr nonlinearity, where the nonlinear parameter $\gamma = \frac{c\omega_p n_2}{n_0^2 V_{\rm eff}}$, $n_2 = 2.6\times10^{-20}$ m^2/W is the Kerr nonlinear coefficient of silica, $n_0 = 1.44$ is the silica refractive index, and $V_{\rm eff} = 370\,\mu$m^2 (from FEM simulation) is the effective mode volume [1–3]. However, compared with the dominant optomechanical effect, the self-phase modulation on the pump wave is negligible in the spiderweb ring resonator. The final term in Eq. (S1) represents the external field coupling with a photon escape rate of $\Gamma_{\rm ep}$.

Assume that the input pump wave consists of an intense continuous wave together with a small time-varying modulation, $A_p = A_{\rm p0} + \delta A_p(t)$. The intracavity field can be written as $a_p = a_{\rm p0} + \delta a_p(t)$, governed by the following equations:

$$\frac{da_{\rm p0}}{dt} = (i\Delta_p - \frac{\Gamma_{\rm tp}}{2})a_{\rm p0} + i\sqrt{\Gamma_{\rm ep}}A_{\rm p0}, \tag{S2}$$

$$\frac{d\delta a_p}{dt} = (i\Delta_p - \frac{\Gamma_{\rm tp}}{2})\delta a_p - ig_{\rm OM}xa_{\rm p0} + i\sqrt{\Gamma_{\rm ep}}\delta A_{\rm p}, \tag{S3}$$

where we have neglected the negligible self-phase modulation for the pump wave. Equation (S2) provides a steady-state solution of

$$a_{\rm p0} = \frac{i\sqrt{\Gamma_{\rm ep}}A_{\rm p0}}{\Gamma_{\rm tp}/2 - i\Delta_p}, \tag{S4}$$

from which we obtain the average pump power dropped into the cavity, $P_{\rm pd}$, given by

$$P_{\rm pd} = \frac{P_{\rm p0}\Gamma_{\rm 0p}\Gamma_{\rm ep}}{\Delta_p^2 + (\Gamma_{\rm tp}/2)^2}, \tag{S5}$$

where $P_{\rm p0} = |A_{\rm p0}|^2$ is the averaged input pump power and $\Gamma_{\rm 0p}$ is the intrinsic photon decay rate of the pump mode. Clearly, to the zeroth order, the relative magnitude of the dropped pump power modulation is directly equal to that of the input modulation:

$$\frac{\delta P_{\rm pd}(t)}{P_{\rm pd}} = \frac{\delta P_p(t)}{P_{\rm p0}}, \tag{S6}$$

where $\delta P_p = A_{\rm p0}^* \delta A_p + A_{\rm p0}\delta A_p^*$ is the time-varying component of the input pump power.

Eq. (S3) leads to a pump-field modulation in the frequency domain of

$$\delta\widetilde{a}_p(\Omega) = \frac{ig_{\rm OM}a_{\rm p0}\widetilde{x}(\Omega) - i\sqrt{\Gamma_{\rm ep}}\delta\widetilde{A}_p(\Omega)}{i(\Delta_p + \Omega) - \Gamma_{\rm tp}/2}, \tag{S7}$$

where $\delta\widetilde{a}_p(\Omega)$, $\widetilde{x}(\Omega)$, and $\delta\widetilde{A}_p(\Omega)$ are Fourier transforms of $\delta a_p(t)$, $x(t)$, and $\delta A_p(t)$, respectively, defined as $\widetilde{B}(\Omega) = \int_{-\infty}^{+\infty} B(t)e^{i\Omega t}dt$. Physically, the first term in Eq. (S7) represents the perturbation induced by the mechanical motion, while the second term represents the effect of direct input modulation.

B. Optical gradient force

The optical gradient force is linearly proportional to the cavity energy as $F_o = -\frac{g_{\rm OM}U_p}{\omega_p}$. With modulation of the pump energy as discussed in the previous section, the gradient force thus consists of two terms, $F_o = F_{o0} + \delta F_o(t)$, where $F_{o0} = -\frac{g_{\rm OM}U_{\rm p0}}{\omega_p}$ is the static force component introduced by the averaged pump energy $U_{\rm p0} = |a_{\rm p0}|^2$, and $\delta F_o(t)$ is the dynamic component related to the pump energy modulation $\delta U_p(t)$, given by

$$\delta F_o(t) = -\frac{g_{\rm OM}\delta U_p}{\omega_p} = -\frac{g_{\rm OM}}{\omega_p}\left[a_{\rm p0}^*\delta a_p(t) + a_{\rm p0}\delta a_p^*(t)\right]. \tag{S8}$$

Substituting Eq. (S7) into Eq. (S8), we find the force modulation is described by this general form in the frequency domain:

$$\delta\widetilde{F}_0(\Omega) = f_o(\Omega)\widetilde{x}(\Omega) + \frac{i\sqrt{\Gamma_{\rm ep}}g_{\rm OM}}{\omega_p}\left[\frac{a_{\rm p0}^*\delta\widetilde{A}_p(\Omega)}{i(\Delta_p+\Omega) - \Gamma_{\rm tp}/2} + \frac{a_{\rm p0}\delta\widetilde{A}_p^*(-\Omega)}{i(\Delta_p-\Omega) + \Gamma_{\rm tp}/2}\right], \tag{S9}$$

where the first term represents the back action introduced by the mechanical motion, with a spectral response $f_0(\Omega)$ given by

$$f_o(\Omega) \equiv -\frac{2g_{\rm OM}^2|a_{\rm p0}|^2\Delta_p}{\omega_p}\frac{\Delta_p^2 - \Omega^2 + (\Gamma_{\rm tp}/2)^2 + i\Gamma_{\rm tp}\Omega}{\left[(\Delta_p+\Omega)^2 + (\Gamma_{\rm tp}/2)^2\right]\left[(\Delta_p-\Omega)^2 + (\Gamma_{\rm tp}/2)^2\right]}. \tag{S10}$$

DOI: 10.1038/NPHOTON.2009.137

C. The squeeze-film effect

The spiderweb ring resonators are separated by a 150-nm gap, which is only about 2.2 times the mean free path in a nitrogen environment (~68 nm). As the ring is ~ 6.3 μm wide, much larger than the ring gap, the nitrogen gas sandwiched in the gap is highly confined by the two silica layers and cannot move freely during the flapping motion of the two rings. The resulting significant pressure differential between the internal and external regions of the paired silica rings functions as a viscous force to damp the mechanical motion. This phenomenon is well-known as the squeeze-film effect, which has a profound impact on the dynamic response of micro/nano-mechanical systems [4]. Apart from the optical gradient force, the squeeze film effect is the dominant mechanism responsible for the dynamic mechanical response of our devices. The associated damping force can be described by a general form of $\widetilde{F}_{\rm sq}(\Omega) = f_{\rm sq}(\Omega)\widetilde{x}(\Omega)$, where $f_{\rm sq}(\Omega)$ represents the spectral response of the squeeze film.

In general, the squeeze film effect is typically described by two theories which work in quite different regimes, depending on the Knudsen number K_n characterizing the ratio between the mean-free path and the gap [4]. In the classical regime with $K_n \ll 1$ where the gas can be considered a continuum, the squeeze-film viscous force for a rectangular plate is well described by $f_{\rm sq}(\Omega) = -k_e(\Omega) + iC_d(\Omega)$, where k_e and C_d represents the spring constant and damping, respectively, induced by the squeeze film. They are given by the following equations [5]

$$k_e(\Omega) = \frac{64\sigma^2 P_a L_0 W_0}{\pi^8 h_0} \sum_{m,n\ odd} \frac{1}{m^2 n^2 \left[(m^2+(n/\eta)^2)^2 + \sigma^2/\pi^4\right]}, \tag{S11}$$

$$C_d(\Omega) = \frac{64\sigma P_a L_0 W_0}{\pi^6 h_0} \sum_{m,n\ odd} \frac{m^2+(n/\eta)^2}{m^2 n^2 \left[(m^2+(n/\eta)^2)^2 + \sigma^2/\pi^4\right]}, \tag{S12}$$

where P_a is the ambient gas pressure, W_0 and L_0 are the width and length of the plate, h_0 is the gap, $\eta = L_0/W_0$ is the aspect ratio of the plate, and σ is the squeeze number given by

$$\sigma(\Omega) = \frac{12\mu_{\rm eff} W_0^2 \Omega}{P_a h_0^2}, \tag{S13}$$

where $\mu_{\rm eff} = \mu/(1+9.638K_n^{1.159})$ is the effective value of the viscosity coefficient μ [6]. Under this model, the squeeze film functions primarily as a damping (or elastic) force when the modulation frequency is below (or above) the cutoff frequency given by

$$\Omega_c = \frac{\pi^2 P_a h_0^2}{12\mu_{\rm eff}} \left(\frac{1}{W_0^2} + \frac{1}{L_0^2}\right). \tag{S14}$$

In contrast, in the free-molecule regime with $K_n \gg 1$ where the interaction between gas molecules is negligible, the squeeze film approximately behaves like a damping force, $f_{sq}(\Omega) = iC_r\Omega$, with C_r given by the following equation [7, 8]

$$C_r = \left(\frac{S}{16\pi h_0}\right) 4P_a L_0 W_0 \sqrt{\frac{2M_m}{\pi \mathscr{R} T}}, \tag{S15}$$

where M_m is the molar mass of gas, T is the temperature, $\mathscr{R}$ is the ideal gas constant, S is the perimeter length of the gap region.

However, our devices have a Knudsen number of $K_n = 0.45$, falling in the crossover regime where neither theory adequately describes the squeeze-film effect [9]. As the device works in the regime between the continuum and free-molecule limit, we heuristically propose that the damping/elastic force of the squeeze film is effectively described by a composite of the two theories:

$$f_{sq}(\Omega) = -k_e(\Omega) + iC_d(\Omega) + i\eta_r C_r \Omega, \tag{S16}$$

with a modified effective coefficient of viscosity $\mu'_{\text{eff}} = \eta_\mu \mu_{\text{eff}}$, where η_r and η_μ are parameters used for a best description of the squeeze-film response in our devices. Detailed analysis shows that $\eta_\mu = 0.7$ and $\eta_r = 0.03$ provides the best fit for our devices. As our devices have a spiderweb geometry, we approximate it with an equivalent rectangular shape with W_0 given by the ring width, L_0 given by the circumference at the ring center, and $S \approx 2L_0$. As shown in the main text, this model provides an accurate description of the squeeze-film effect in our devices.

Although the intrinsic mechanical frequency of the 54 μm spiderweb structure is 694 kHz (indicated by FEM simulation), Fig. 4(d) in the main text shows a minimum dynamic frequency response of 6 MHz, dominated by the squeeze-film damping. Interestingly, although squeeze-film damping is generally detrimental in other micro/nanomechanical systems [4, 10], it is beneficial in this case, as it helps to extend the modulation bandwidth for wavelength routing.

D. Actuated mechanical motions

With the optical gradient force and the squeeze-film damping force, the mechanical motion of the cavity satisfies the following equation:

$$\frac{d^2x}{dt^2} + \Gamma_m \frac{dx}{dt} + \Omega_m^2 x = \frac{1}{m_{\text{eff}}}(F_o + F_{sq} + F_T) = \frac{1}{m_{\text{eff}}}(F_{o0} + \delta F_o + F_{sq} + F_T), \tag{S17}$$

where m_{eff} is the effective motional mass of the flapping mechanical mode, and Ω_m and Γ_m are intrinsic mechanical frequency and damping rate, respectively. F_T is the thermal Langevin force

DOI: 10.1038/NPHOTON.2009.137

responsible for the thermal Brownian motion, a Markovin process with the following correlation function:

$$\langle F_T(t)F_T(t+\tau)\rangle = 2m_{\rm eff}\Gamma_m k_B T\,\delta(\tau), \tag{S18}$$

where k_B is Boltzmann's constant.

As the squeeze-film viscous force is zero at $\Omega = 0$, the squeeze gas film impacts only the dynamic response of mechanical motion. Equation (S17) shows clearly that the static mechanical displacement is actuated only by the static component of the optical force given by

$$x_0 = \frac{|F_{o0}|}{m_{\rm eff}\Omega_m^2} = \frac{g_{\rm om}U_{\rm p0}}{k_m\omega_p} = \frac{g_{\rm om}P_{\rm pd}}{k_m\omega_p\Gamma_{0\rm p}}, \tag{S19}$$

where $k_m = m_{\rm eff}\Omega_m^2$ is the intrinsic spring constant of the spiderweb structure. With a specifically designed extremely small spring constant, x_0 can be quite significant for a given dropped power. As a result, the cavity resonance can be tuned by a significant magnitude of $g_{\rm OM}x_0$. This is the primary mechanism responsible for the resonance tuning demonstrated in the main text. On the other hand, such a static mechanical displacement primarily changes the equilibrium position of the mechanical motion. It is convenient to remove this component in Eq. (S17) by defining $x' = x - x_0$, since both the squeeze-film damping force and dynamic component of the optical force affect only the dynamics of x'.

Substituting Eqs. (S9), (S10), (S16) into Eq. (S17) in the frequency domain, we find that the squeeze-film damping force and the backaction term of optical force primarily change the values of the resonant frequency and damping rate of the mechanical motions. Define

$$\mathscr{L}(\Omega) \equiv \Omega_m^2 - \Omega^2 - i\Gamma_m\Omega - \frac{f_o(\Omega)}{m_{\rm eff}} - \frac{f_{\rm sq}(\Omega)}{m_{\rm eff}}, \tag{S20}$$

the mechanical displacement is thus given by

$$\widetilde{x}(\Omega) = \frac{\widetilde{F}_T(\Omega)}{m_{\rm eff}\mathscr{L}(\Omega)} + \frac{i\sqrt{\Gamma_{\rm ep}}g_{\rm OM}}{m_{\rm eff}\omega_p\mathscr{L}(\Omega)}\left[\frac{a_{\rm p0}^*\delta\widetilde{A}_p(\Omega)}{i(\Delta_p+\Omega)-\Gamma_{\rm tp}/2} + \frac{a_{\rm p0}\delta\widetilde{A}_p^*(-\Omega)}{i(\Delta_p-\Omega)+\Gamma_{\rm tp}/2}\right], \tag{S21}$$

where we have dropped the prime notation of x' for simplicity.

The first term in Eq. (S21) represents the thermal Brownian motion while the second term describes the motions actuated by the pump modulation. In the absence of pump modulation, the mechanical motion is dominated by the Brownian motion. By using Eq. (S18), we find the spectral density of thermal mechanical displacement has the form

$$\mathscr{S}_x(\Omega) = \frac{2\Gamma_m k_B T}{m_{\rm eff}|\mathscr{L}(\Omega)|^2}. \tag{S22}$$

Equations (S9), (S10), and (S20) show that one dominant effect of the pump energy inside the cavity is to increase the mechanical rigidity, the so-called optical spring effect. In most cases, $\mathscr{L}(\Omega)$ can be well approximated by $\mathscr{L}(\Omega) \approx (\Omega'_m)^2 - \Omega^2 - i\Gamma'_m\Omega$ with a new mechanical resonance Ω'_m and damping rate Γ'_m affected by the optical force. Equation (S22) thus leads to a variance of the thermal mechanical displacement given by

$$\langle(\delta x)^2\rangle = \frac{1}{2\pi}\int_{-\infty}^{+\infty} \mathscr{S}_x(\Omega)d\Omega = \frac{k_B T\Gamma_m}{k'_m\Gamma'_m} \approx \frac{k_B T}{k'_m}, \tag{S23}$$

where $k'_m = m_{\text{eff}}(\Omega'_m)^2$ is the effective spring constant and the approximation in the final term assumes a negligible change in the mechanical linewidth. Clearly, the increase of the mechanical resonance frequency through the optical spring effect dramatically suppresses the magnitude of the thermal mechanical displacement and its perturbation of the cavity resonance, as shown clearly in the main text.

In the presence of pump modulation, the mechanical motion is primarily dominated by the dynamic optical force rather than the actuation from the thermal Langevin force, and the first term is negligible compared with the second term in Eq. (S21). We focus on this situation in the following discussion, neglecting the thermal Brownian term.

E. Cavity response of the probe mode

The probe wave inside the cavity is governed by a dynamic equation similar to Eq. (S1):

$$\frac{da_s}{dt} = (i\Delta_s - \frac{\Gamma_{\text{ts}}}{2})a_s - ig_{\text{OM}}xa_s + 2i\gamma|a_p|^2a_s + i\sqrt{\Gamma_{\text{es}}}A_{\text{s}}, \tag{S24}$$

except that the Kerr-nonlinear term now describes the cross-phase modulation from the pump wave. With the perturbations induced by the pump modulation, similar to the previous discussion of the pump wave, the intracavity probe field can be written as $a_s = a_{\text{s0}} + \delta a_s(t)$, governed by the following equations:

$$\frac{da_{\text{s0}}}{dt} = (i\Delta_s - \frac{\Gamma_{\text{ts}}}{2})a_{\text{s0}} + 2i\gamma U_{\text{p0}}a_{\text{s0}} + i\sqrt{\Gamma_{\text{es}}}A_{\text{s}}, \tag{S25}$$

$$\frac{d\delta a_s}{dt} = (i\Delta_s - \frac{\Gamma_{\text{ts}}}{2})\delta a_s + 2i\gamma U_{\text{p0}}\delta a_{\text{s}} - ig_{\text{OM}}xa_{\text{s0}} + 2i\gamma\delta U_p a_{\text{s0}}, \tag{S26}$$

where we have assumed the probe input is a continuous wave with a power of $P_s = |A_s|^2$. The second terms of Eqs. (S25) and (S26) represent the static cavity tuning introduced by cross-phase modulation, which can be included in the cavity tuning term Δ_s for simplicity. In general, it is

DOI: 10.1038/NPHOTON.2009.137

negligible compared with the cavity linewidth at the power level used for exciting optomechanical effects, leading to $2\gamma U_{\mathrm{p0}} \ll \Gamma_{\mathrm{tp}}, \Gamma_{\mathrm{ts}}$.

Equation (S25) provides a steady-state solution of

$$a_{\mathrm{s0}} = \frac{i\sqrt{\Gamma_{\mathrm{es}}}A_{\mathrm{s}}}{\Gamma_{\mathrm{ts}}/2 - i\Delta_s}, \tag{S27}$$

and Eq. (S26) results in a probe-field modulation in the frequency domain of

$$\delta\widetilde{a}_s(\Omega) = \frac{ia_{\mathrm{s0}}\left[g_{\mathrm{OM}}\widetilde{x}(\Omega) - 2\gamma\delta\widetilde{U}_p(\Omega)\right]}{i(\Delta_s + \Omega) - \Gamma_{\mathrm{ts}}/2}, \tag{S28}$$

where $\delta\widetilde{U}_p(\Omega)$ is the Fourier transform of $\delta U_p(t)$. As the transmitted field of the probe is given by $A_{\mathrm{Ts}} = A_s + i\sqrt{\Gamma_{\mathrm{es}}}a_s$, the modulation of the transmitted probe power thus takes the form

$$\delta P_{\mathrm{Ts}} = i\sqrt{\Gamma_{\mathrm{es}}}(A^*_{\mathrm{0s}}\delta a_s - A_{\mathrm{0s}}\delta a^*_s), \tag{S29}$$

where $A_{\mathrm{0s}} = A_s + i\sqrt{\Gamma_{\mathrm{es}}}a_{\mathrm{s0}}$ is the transmitted probe wave in the absence of modulation. By use of Eqs. (S7), (S21), (S27) and (S28), we find that the power spectrum of the transmitted probe modulation is given by the following equation:

$$\frac{|\delta\widetilde{P}_{\mathrm{Ts}}(\Omega)|^2}{P_s^2} = \left|\frac{g_{\mathrm{OM}}^2}{m_{\mathrm{eff}}\omega_p\mathscr{L}(\Omega)} + 2\gamma\right|^2 \frac{P_{\mathrm{pd}}^2}{\Gamma_{\mathrm{0p}}^2}\frac{|\delta\widetilde{P}_{\mathrm{pd}}(\Omega)|^2}{P_{\mathrm{pd}}^2}\frac{4\Gamma_{\mathrm{es}}^2\Gamma_{\mathrm{0s}}^2\Delta_s^2}{[\Delta_s^2 + (\Gamma_{\mathrm{ts}}/2)^2]^4}, \tag{S30}$$

where Γ_{0s} is the intrinsic photon decay rate of the probe mode, and $\delta\widetilde{P}_{\mathrm{Ts}}(\Omega)$ and $\delta\widetilde{P}_{\mathrm{pd}}(\Omega)$ are the Fourier transforms of $\delta P_{\mathrm{Ts}}(t)$ and $\delta P_{\mathrm{pd}}(t)$, respectively. To obtain Eq. (S30), we have used Eq. (S6) to relate the dropped pump power to the input, and have also taken into account the fact that the Kerr effect is relatively small, such that $2\gamma U_{\mathrm{p0}} \ll \Gamma_{\mathrm{tp}}$. We also assume the cavity is in the sideband-unresolved regime with $\Omega_m \ll \Gamma_{\mathrm{tp}}, \Gamma_{\mathrm{ts}}$. The modulation spectra given in the main text are defined as

$$\rho(\Omega) \equiv \frac{|\delta\widetilde{P}_{\mathrm{Ts}}(\Omega)|^2/P_s^2}{|\delta\widetilde{P}_{\mathrm{pd}}(\Omega)|^2/P_{\mathrm{pd}}^2}. \tag{S31}$$

For a better comparison of the dynamic-backaction induced variations on the probe modulation, the modulation spectra shown in Fig. 4d of the main text are normalized by a factor corresponding to the ratio of the dropped power for each curve relative to the maximum dropped power. Therefore, the plot modulation spectra are given by

$$\rho'(\Omega) \equiv \rho(\Omega)\frac{P_{\mathrm{pd0}}^2}{P_{\mathrm{pd}}^2} = \frac{|\delta\widetilde{P}_{\mathrm{Ts}}(\Omega)|^2/P_s^2}{|\delta\widetilde{P}_{\mathrm{pd}}(\Omega)|^2/P_{\mathrm{pd0}}^2}, \tag{S32}$$

where $P_{\mathrm{pd0}} = 0.85$ mW is the maximum drop power used in Fig. 4d.

The derivations above take into account only the flapping mechanical mode, since it is most strongly actuated by the optical gradient force. In general, there are many mechanical resonances for the spiderweb resonators, but weakly coupled to the optical waves inside the cavity. In this case, following the same procedure above, it is easy to show that the spectral response of probe modulation now becomes

$$\rho(\Omega) = \left| 2\gamma + \sum_j \frac{g_j^2}{m_{\mathrm{j}}\omega_p \mathscr{L}_j(\Omega)} \right|^2 \frac{P_{\mathrm{pd}}^2}{\Gamma_{0\mathrm{p}}^2} \frac{4\Gamma_{\mathrm{es}}^2 \Gamma_{0\mathrm{s}}^2 \Delta_s^2}{[\Delta_s^2 + (\Gamma_{\mathrm{ts}}/2)^2]^4}, \tag{S33}$$

where g_j, m_j, and $\mathscr{L}_j(\Omega)$ are optomechanical coupling coefficient, effective motional mass, and the spectral response of mechanical motions, respectively, for the j^{th} mechanical mode. For those weakly actuated mechanical modes, $\mathscr{L}_j(\Omega) = \Omega_{\mathrm{mj}}^2 - \Omega^2 - i\Gamma_{\mathrm{mj}}\Omega$ where Ω_{mj} and Γ_{mj} are the resonance frequency and damping rate of the j^{th} mechanical mode. Equation (S33) was used to describe the modulation spectrum shown in Fig. 4(d).

II. ANTI-CROSSING OF TWO PROBE MODES

The anti-crossing between the two probe modes when they approache each other is primarily due to the internal coupling between the two cavity modes, which can be described by a simple theory as follows. Assume two cavity resonances located at ω_{01} and ω_{02}. For an input probe wave at ω, the two cavity modes are excited through the following equations:

$$\frac{da_1}{dt} = (i\Delta_1 - \frac{\Gamma_{\mathrm{t1}}}{2})a_1 + i\beta a_2 + i\sqrt{\Gamma_{\mathrm{e1}}}A_{\mathrm{in}}, \tag{S34}$$

$$\frac{da_2}{dt} = (i\Delta_2 - \frac{\Gamma_{\mathrm{t2}}}{2})a_2 + i\beta a_1 + i\sqrt{\Gamma_{\mathrm{e2}}}A_{\mathrm{in}}, \tag{S35}$$

where $\Delta_j = \omega - \omega_{0\mathrm{j}}$ represents the cavity detuning of the j^{th} mode, and β is the optical coupling coefficient between the two cavity modes. With a continuous-wave input, the steady state of Eqs. (S34) and (S35) is given by the following solution

$$a_1 = \frac{-iA_{\mathrm{in}}\left[(i\Delta_2 - \Gamma_{\mathrm{t2}}/2)\sqrt{\Gamma_{\mathrm{e1}}} - i\beta\sqrt{\Gamma_{\mathrm{e2}}}\right]}{(i\Delta_1 - \Gamma_{\mathrm{t1}}/2)(i\Delta_2 - \Gamma_{\mathrm{t2}}/2) + \beta^2}, \tag{S36}$$

$$a_2 = \frac{-iA_{\mathrm{in}}\left[(i\Delta_1 - \Gamma_{\mathrm{t1}}/2)\sqrt{\Gamma_{\mathrm{e2}}} - i\beta\sqrt{\Gamma_{\mathrm{e1}}}\right]}{(i\Delta_1 - \Gamma_{\mathrm{t1}}/2)(i\Delta_2 - \Gamma_{\mathrm{t2}}/2) + \beta^2}. \tag{S37}$$

DOI: 10.1038/NPHOTON.2009.137

As the transmitted field from the cavity is given by $A_T = A_{in} + i\sqrt{\Gamma_{e1}}a_1 + i\sqrt{\Gamma_{e2}}a_2$, the cavity transmission thus has the following equation

$$T \equiv \frac{|A_T|^2}{|A_{in}|^2} = \left| \frac{(i\Delta_1 - \frac{\Gamma_{01}-\Gamma_{e1}}{2})(i\Delta_2 - \frac{\Gamma_{02}-\Gamma_{e2}}{2}) + (\beta - i\sqrt{\Gamma_{e1}\Gamma_{e2}})^2}{(i\Delta_1 - \Gamma_{t1}/2)(i\Delta_2 - \Gamma_{t2}/2) + \beta^2} \right|^2 . \quad \text{(S38)}$$

III. QUANTIFYING THE OPTICAL QUALITY FACTOR

The extremely small intrinsic spring constant of the spiderweb resonator leads to significant thermal Brownian mechanical motion and introduces considerable fluctuations on the cavity transmission spectrum, as shown in Fig. 4a in the main text. This makes it difficult to measure the optical Q factor of a cavity resonance. As discussed previously, the thermal Brownian mechanical motion can be significantly suppressed through the optical spring effect. This feature provides an elegant way to accurately characterize the optical Q of a cavity mode, by launching a relatively intense wave at a different resonance to suppress the perturbations induced by the thermal mechanical motions. Moreover, a complete theory developed previously [11] was used to describe the linear cavity transmission with the inclusion of the optomechanical effect.

IV. CALIBRATION OF THERMO-OPTIC AND THERMO-MECHANICAL CONTRIBUTIONS

The thermo-optical effect on the resonance tuning was calibrated by using another identical device on the same sample. To isolate the thermo-optic effect from the optomechanical effect, we caused the two rings to stick together through the van der Waals force, so the flapping mechanical motion was completely eliminated. Testing was performed on a cavity mode at 1552 nm using exactly the same conditions as for the wavelength routing measurements in the main text. A power of 2.1 mW dropped into the cavity introduces a maximum resonance red tuning by 0.23 nm, corresponding to a tuning rate of 0.11 nm/mW (13.8 GHz/mW), about 4% of the total tuning rate recorded experimentally.

The thermo-optic resonance tuning indicates a maximum temperature change of 21 K in the resonator. FEM simulations show that such a temperature variation of the resonator introduces a ring-gap change by only about 10 pm, shown by the differential displacement of the top and bottom rings in Fig. S1. Therefore, thermally induced static mechanical deformation has only a negligible contribution of 0.06% of the experimentally recorded wavelength tuning.

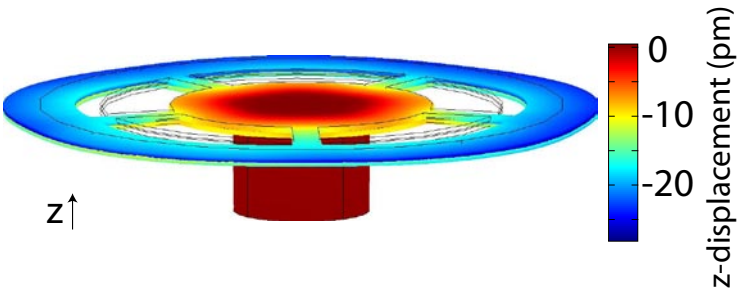

FIG. S1: **Thermomechanical deflection of a spiderweb resonator**. FEM simulation illustrating the z-displacement of a 54 μm spiderweb resonator under the 21 K temperature differential between substrate and ring induced by 2.1 mW dropped optical power.

The negligible contributions of both thermo-optic and thermo-mechanical effects are double confirmed by the pump-probe modulation spectra shown in Fig. 4d and e in the main text, as discussed in detail in the main text.

[1] G. P. Agrawal, *Nonlinear Fiber Optics 4th ed* (Academic Press, New York, NY, 2007).

[2] Q. Lin, O. Painter, and G. Agrawal, Opt. Express **15**, 16604 (2007).

[3] Q. Lin, T. Johnson, R. Perahia, C. Michael, and O. Painter, Opt. Express **16**, 10596 (2008).

[4] M. Bao and H. Yang, Sens. Actuators, A **136**, 3 (2007), and references therein.

[5] J. J. Blech, J. Tribol. **105**, 615 (1983).

[6] T. Veijola, H. Kuisma, J. Lahdenperä, and T. Ryhänen, Sens. Actuators, A **48**, 239 (1995).

[7] R. Christian, Vacuum **16**, 175 (1966).

[8] M. Bao, H. Yang, H. Yin, and Y. Sun, J. Micromech. Microeng. **12**, 341 (2002).

[9] R. Bhiladvala and Z. Wang, Phys. Rev. E **69**, 036307 (2004).

[10] S. S. Verbridge, J. M. Parpia, R. B. Reichenbach, L. M. Bellan, and H. G. Craighead, J. Appl. Phys. **99**, 124304 (2006).

[11] Q. Lin, J. Rosenberg, X. Jiang, K. J. Vahala, and O. Painter, submitted for publication.